Cardiac Myosin-Binding Protein C Modulates the Tuning of the Molecular Motor in the Heart

Yves Lecarpentier,*†‡ Nicolas Vignier,¶§ Patricia Oliviero,¶‖ Aziz Guellich,*‖ Lucie Carrier,¶§** and Catherine Coirault†¶§

*INSERM, U689, Cardiovascular Research Center, Paris, France; †Assistance Publique Hôpitaux de Paris, Hôpital Bicêtre, Service d'Explorations Cardio-Respiratoires, Le Kremlin-Bicetre, France; ‡University Paris 11, Le Kremlin-Bicêtre, France; ¶INSERM, U582, Institut de Myologie, Paris, France; §UPMC Univ Paris 06, UMR-S582, IFR14, Paris, France; ‖University Paris 7, Paris, France; and **Institute of Experimental and Clinical Pharmacology and Toxicology, University Medical Center Hamburg-Eppendorf, Hamburg, Germany

ABSTRACT Cardiac myosin binding protein C (cMyBP-C) is an important regulator of cardiac contractility. Its precise effect on myosin cross-bridges (CBs) remains unclear. Using a cMyBP-C$^{-/-}$ mouse model, we determined how cMyBP-C modulates the cyclic interaction of CBs with actin. From papillary muscle mechanics, CB characteristics were provided using A. F. Huxley's equations. The probability of myosin being weakly bound to actin was higher in cMyBP-C$^{-/-}$ than in cMyBP-C$^{+/+}$. However, the number of CBs in strongly bound, high-force generated state and the force generated per CB were lower in cMyBP-C$^{-/-}$. Overall CB cycling and the velocity of CB tilting were accelerated in cMyBP-C$^{-/-}$. Taking advantage of the presence of cMyBP-C in cMyBP-C$^{+/+}$ myosin solution but not in cMyBP-C$^{-/-}$, we also analyzed the effects of cMyBP-C on the myosin-based sliding velocity of actin filaments. At baseline, sliding velocity and the relative isometric CB force, as determined by the amount of α-actinin required to arrest thin filament motility, were lower in cMyBP-C$^{-/-}$ than in cMyBP-C$^{+/+}$. cAMP-dependent protein kinase-mediated cMyBP-C phosphorylation further increased the force produced by CBs. We conclude that cMyBP-C prevents inefficient, weak binding of the myosin CB to actin and has a critical effect on the power-stroke step of the myosin molecular motor.

INTRODUCTION

Cardiac contraction involves the cyclic interaction of the myosin cross-bridges (CBs) with the actin filaments. This is a highly regulated process that couples ATP hydrolysis to motility and force generation (1,2). Whereas low Ca^{2+} levels prevent actin-myosin interactions in diastole, the rise in intracellular Ca^{2+} during systole initiates a series of conformational changes that cause the myosin CBs to bind to activated thin filaments. Binding occurs in one of two ways, either weakly or strongly (3,4). The initial weak binding to actin isomerizes to a strongly bound, force-generating step often referred to as the power-stroke, which moves the actin filament past the myosin filaments and generates force. This is associated with rotation of the light-chain binding region and the release of the ATP hydrolysis products. The association of a new ATP molecule weakens the binding again, and the attached CB rapidly dissociates from actin. The nucleotide is then hydrolyzed, the conformational change reverses, and the myosin CB can reattach to actin (4,5).

Cardiac myosin-binding protein C (cMyBP-C), for which mutations are one of the major causes of familial hypertrophic cardiomyopathy (FHC) (for reviews see (6,7)), is a large thick filament-associated protein that consists of 11 modules labeled C0 to C10 from the N- to the C-terminus. cMyBP-C binds to the heavy meromyosin through its C10 domain whereas the MyBP-C motif, a phosphorylable motif linking the C1 and C2 domains, binds to the myosin subfragment S2 (8) close to the lever arm domain of myosin. Phosphorylation of the MyBP-C motif results in a rearrangement of the myosin head and the structure of the thick filament (9). cMyBP-C also binds titin via domains C8-C10 (10) and actin in the Pro-Ala rich sequence between the C0 and C1 domains (11).

There is increasing evidence that cMyBP-C plays a critical role in the regulation of cardiac contractility. It has been proposed that cMyBP-C is involved in the activation process of the cardiac sarcomere (12–15). Accordingly, previous studies suggest that cMyBP-C modulates myofilament Ca^{2+} sensitivity (13,16–18) probably via sarcomere length-dependent activation (18). In addition, it is assumed that ablation of cMyBP-C relieves a physical constraint on myosin, which then allows myosin to move radially from the surface of the thick filament. This would increase the likelihood of CB formation (14,19) and accelerated CB cycle kinetics (15,17,20). However, questions remain as to which step cMyBP-C regulates in the actin-myosin cycle and how potential modifications of the myosin CB cycle contribute to the cardiac dysfunction.

This study was undertaken to determine the functional effects of cMyBP-C on the essential states of interaction of myosin heads with actin so as to understand how cMyBP-C interferes with the actin-myosin CB cycle. To this end, we used a homozygous cardiac cMyBP-C-null mice (cMyBP-C$^{-/-}$) based upon the targeted deletion of the transcription initiation site and exons 1–2 of the mouse cMyBP-C gene (21,22).

Submitted December 13, 2007, and accepted for publication March 10, 2008.

Address reprint requests to Dr. C. Coirault, E-mail: c.coirault@institut-myologie.org.

Editor: Cristobal G. dos Remedios.

0006-3495/08/07/720/09 $2.00

doi: 10.1529/biophysj.107.127787

MATERIALS AND METHODS

Mouse models

Cardiac cMyBP-C-null mice were generated previously (21) and maintained in a breeding colony. Briefly, the mouse model was based upon the targeted deletion of the transcription initiation site and exons 1–2 of the mouse cMyBP-C gene (21). In this study, cMyBP-C$^{+/+}$ and cMyBP-C$^{-/-}$ ($n = 20$ in each group) mice of either sex were studied at 16 weeks of age. Electrophoretic and Western blot analyses confirmed the absence of cMyBP-C in the null mice (21). Experiments were also performed in a cMyBP-C$^{+/+}$ mouse model of either sex fed an iodine-deficient, 0.15% 6-*n*-propyl-2-thiouracil (PTU) diet before study (cMyBP-C$^{+/+}$+PTU, $n = 12$). Duration of PTU therapy was determined so as to obtain similar shift in the myosin isoform pattern in cMyBP-C$^{+/+}$+PTU and cMyBP-C$^{-/-}$ mice. All procedures conformed to the Guide for Care and Use of Laboratory Animals and have been approved by the local committee of our institution.

Papillary muscle preparations

Mechanical experiments were performed on LV papillary muscle as previously described (23). Briefly, after an IP injection of sodium pentobarbital, the heart was rapidly excised and placed in a physiological solution. The LV was opened under a dissection microscope and the anterior papillary muscle was carefully dissected. The muscle was then placed in a circulating organ bath containing modified Krebs-Henseleit buffer solution (24) with 5% fetal calf serum. The solution was bubbled with 95% O_2 and 5% CO_2 and maintained at 29°C and pH 7.4. One end of the extremity of the papillary muscle was held by a stationary clip and the other was maintained with another clip attached to an isotonic electromagnetic force-transducer lever. After an equilibration period of 30 min, muscle was supramaximally stimulated using two platinum electrodes at the optimal force-frequency response, i.e., at a frequency of six stimulations/min. Experiments were performed at L_{max}, the initial muscle length at which active isometric tension was maximum. The CSA was calculated as previously described (25).

Papillary muscle mechanical parameters

Muscle mechanical parameters and parameters determined from A. V. Hill's equation were determined over the whole load continuum (24,26). During the contraction phase, we recorded the maximum unloaded shortening velocity (V_{max}, in $L_{max}.s^{-1}$) from the zero-load contraction; the maximum extent of shortening (δ_L, in % L_{max}) and the time-to-peak shortening (TPS) of the contraction loaded with preload only; the peak isometric tension, i.e., peak force normalized per CSA (P_{max}, in $mN.mm^{-2}$); and the positive peak of isometric tension derivative of the fully isometric contraction ($+dP/dt$, $mN.mm^{-2}.s^{-1}$). To characterize the relaxation process, we measured the peak lengthening velocity at preload (V_L, in $L_{max}.s^{-1}$) and the peak rate of tension decline of the fully isometric contraction ($-dP/dt$, in $mN.s^{-1}.mm^{-2}$). The hyperbolic tension-velocity (P-V) relationship was derived from the peak velocity of 8–10 isotonic after loaded contractions and was fitted according to Hill's equation $(P+a)(V+b) = [P_{max}+a]b$ where $-a$ and $-b$ are the asymptotes of the hyperbola as determined by multilinear regression (26). The G curvature of the P-V curve is equal to $P_{max}/a = V_{max}/b$ (26).

CB kinetics and probabilities of CB steps

The actomyosin interaction was analyzed according to a multistate conformational model based on Huxley's original CB model (27) and consistent with recent models of muscle contraction (4,5). Initial CB attachment occurs with a rate constant f_1 and leads to the formation of a weakly attached, low-force state (AM-ADP-Pi). After transition to a strongly bound, high-force state, the attached CB AM-ADP-Pi executes a power-stroke, causing a relative displacement of the actin filament. This state, triggered by the release of Pi leads to the formation of AM-ADP. The release of ADP occurs after the power-stroke step and leads to the formation of AM. Then, the binding of one ATP molecule to the myosin head causes the actomyosin complex to detach (A+M-ATP). The rate constant for cross-bridge detachment was g_2. ATP hydrolysis then occurs (M*-ADP-Pi) where M* is myosin in a refractory state (28). This leads to a conformational change in myosin (M-ADP-Pi) allowing a new cycle to begin.

A. F. Huxley's equations (27) were used to calculate the total duration of the CB cycle under isometric conditions (in milliseconds); the duration of the power-stroke step (in milliseconds); CB velocity during the stroke (v_o, in $\mu m.s^{-1}$); the elementary force per single CB (in piconewtons); the number of active CBs, peak efficiency (Effmax, in %); the peak value of the rate constant for CB attachment during the stroke step (f_1, in s^{-1}); and the peak value of the rate constant for CB detachment during (g_1, in s^{-1}) and after the stroke step (g_2, in s^{-1}) (24,29). The free energy of ATP hydrolysis (e) was chosen to be equal to 5.1×10^{-20} J (24,29), the distance ℓ between two actin sites was equal to 14.3 nm (27) and h, the translocation distance of the actin filament per ATP hydrolysis produced by the swing of the myosin head was equal to 5 nm (30). In cycling myosin molecules, the probability of actomyosin states was calculated from the ratio of their time duration and the time cycle (1). Briefly, the probability of cycling myosin being in the detached state M-ATP is given by $P_{D1} = (1/g_2)$/time cycle. The probability of actomyosin being in a weakly attached, low-force state (AM*-ADP-Pi) is given by $P_{A1} = (1/f_1)$/time cycle. The probability of actomyosin being in a strongly-bound high force state (AM-ADP state) is PA_2 = time stroke/time cycle (1).

In vitro motility assays

Mouse LV myosin was isolated as previously described (23,31) and used within 48 h. To determine whether cMyBP-C affects myosin mechanical properties, we took advantage of the fact that cMyBP-C is a classic contaminant of myosin preparation (32). SDS-Page electrophoresis was used to assess the purity of myosin and the presence of cMyBP-C was detected by Western-blot using a polyclonal antibody directed against the cMyBP-C motif (generous gift from Wolfgang Linke, Münster, Germany). F-actin was prepared from rabbit skeletal muscle by standard methods (33) and fluorescently labeled with phalloidin FluoProbes 547 (Interchim, Montlucon, France). Motility assays were carried out at 29°C as previously described (31,34). In brief, myosin (100 μg/ml in high salt buffer containing 40 mmol/L potassium phosphate buffer, 1 mol/L KCl, 2 mmol/L dithiothreitol, and 4 mM $MgCl_2$, pH 6.5) was plated onto a nitrocellulose-coated glass coverslip. Unbound myosin was washed out with low salt buffer (25 mmol/L KCl, 25 mmol/L imidazole, 4 mmol/L $MgCl_2$, 1 mmol/L dithiothreitol, and 1 mmol/L ethylene glycol-bis (β-aminoethyl ether, pH 7.4) supplemented with 0.5 mg/ml bovine serum albumin. Unlabeled F-actin filaments were used to eliminate nonfunctional myosin molecules (35). Motility of fluorescently labeled actin filaments (20 nmol/L) was initiated by adding 2 mmol MgATP with an oxygen-scavenger enzyme system (20 mmol dithiothreitol, 0.02 mg/ml catalase, 0.1 mg/ml glucose oxidase, 3 mg/ml glucose). The movement of the actin filaments was observed under a Zeiss epifluorescence microscope (model No. 200, 100/1.30 lens, Axiovert, Jena, Germany) equipped with an intensified camera (model No. C 2400, Hamamatsu, Hamamatsu City, Japan) and recorded on videotape. The mean velocities of each filament were analyzed using N. J. Carter's freeware RETRAC program.

Effects of cAMP-dependent protein kinase (PKA)

To assess the effects of cMyBP-C phosphorylation on myosin mechanical properties, myosin solution was preincubated for 15 min at 22°C with 10 μmol of catalytic subunit of cAMP-dependent protein kinase (PKA) (Sigma Chemical, St. Louis, MO) before use in the motility assay. Phosphorylation under basal conditions and after PKA treatment was determined by Western-blot using a polyclonal antibody directed against the phosphorylated Ser^{82} of

cMyBP-C forms (ALX-215-057, Axxora, San Diego, CA) (36). Immunodetection was revealed with the ECL system (ECL-Plus kit, Amersham Pharmacia, Piscataway, NJ).

Relative force of myosin molecules

Relative isometric force was determined by using α-actinin as an internal load (37,38). In brief, myosin was adhered to the nitrocellulose-coated coverslip as described above. Alpha-actinin was then attached to the coverslip surface (15–100 μg/ml in low-salt buffer), followed by a bovine serum albumin wash (0.5 mg/ml in low-salt buffer). Unregulated actin filaments (20 nmol/L) were then added to the motility surface. Motility was initiated by the addition of 2 mmol MgATP with the oxygen-scavenger enzyme system, as described above. As α-actinin avidly binds to actin, the motion of the thin filament is impeded by the α-actinin adhered to the surface. The load placed on a thin filament is a function of the relative concentrations of the force generator (myosin) and the motion inhibitor (α-actinin). The amount of α-actinin adhered to the motility surface was gradually increased until motility was completely arrested, thus indicating an isometric state. Relative isometric force was then defined as the minimum amount of α-actinin needed to completely arrest thin filament motility.

Myosin isoform composition

Myosin isoform composition was determined on purified myosin obtained from both LV and papillary muscle and stored in 50% glycerol. Alpha- and β-myosin isoforms were separated on 8% polyacrylamide gels containing 10% glycerol (23). SDS-PAGE was performed in a Mini-Protean II Dual Slab Cell electrophoresis system (BioRad, Hercules, CA) for 16 h at 4°C and 70 V. Gels were stained with Coomassie blue and quantification of α- and β-myosin isoforms were quantified using Image Gauge software.

Statistical analysis

Data are expressed as mean ± SE. After analysis of variance, differences in selected measurements between groups were evaluated by Fisher's test. All comparisons were two-tailed and a p-value < 0.05 was considered statistically significant.

RESULTS

Mechanical performance of in vitro LV papillary muscle

Contractile mechanical parameters of LV papillary muscles are given in Table 1. Compared with cMyBP-C$^{+/+}$, contractile performance was severely depressed in cMyBP-C$^{-/-}$, as attested by a reduction in maximum extent of shortening (δ_L), maximum unloaded shortening velocity (V_{max}), total tension (P_{max}), and $+dP/dt$ (−58%, −45%, −57%, and −59% respectively, each $p < 0.05$). Peak shortening occurred significantly earlier in cMyBP-C$^{-/-}$ than in cMyBP-C$^{+/+}$ (Table 1; $p < 0.05$). Interestingly, depressed contractile performance in cMyBP-C$^{-/-}$ mice was associated with severe impairment of relaxation (Table 1), as attested by slower $-dP/dt$ and maximum lengthening velocity (V_L) in cMyBP-C$^{-/-}$ compared with cMyBP-C$^{+/+}$ (−67% and −67%, respectively, each $p < 0.001$).

TABLE 1 Performance of LV papillary muscles during the contraction and relaxation phases

	cMyBP-C$^{+/+}$	cMyBP-C$^{-/-}$
Contraction parameters		
δ_L, % L_{max}	6.9 ± 0.7	2.9 ± 0.8*
V_{max}, L_{max}/s	2.4 ± 0.3	1.3 ± 0.3†
P_{max}, mN/mm^2	24.5 ± 2.2	10.5 ± 1.4*
$+dP/dt$, mN/mm^2/s	125.2 ± 19.8	51.4 ± 11.9*
TPS, ms	120 ± 4	105 ± 5†
Relaxation parameters		
$-dP/dt$, mN/mm^2/s	206.5 ± 23.4	68.8 ± 14*
V_L, L_{max}/s	1.2 ± 0.1	0.4 vs. 0.1*

δ_L, maximum extent of shortening at preload; V_{max}, maximum shortening velocity at zero-load; P_{max}, total isometric tension; $+dP/dt$, positive peak derivative of isometric tension; *TPS*, time-to-peak shortening at preload; $-dP/dt$, negative peak derivative of isometric tension; V_L, peak lengthening velocity at preload. Values are means ± SE.
*$p < 0.01$, $N = 8$ in each group.
†$p < 0.05$;

Cyclical interactions of the myosin CB with actin in papillary muscles

We used a multistate conformational model based on A. F. Huxley's original CB model (27) to characterize CB properties in cMyBP-C$^{+/+}$ and cMyBP-C$^{-/-}$ papillary muscles. The number of active CBs, i.e., CBs involved in the power-stroke during isometric contraction was almost 45% lower in cMyBP-C$^{-/-}$ than in cMyBP-C$^{+/+}$ ($p < 0.001$, Fig. 1 *A*). Moreover, the force produced per CB was 23% lower in cMyBP-C$^{-/-}$ than in cMyBP-C$^{+/+}$ mice (Fig. 1 *B*, $p < 0.001$). This was associated with a 29% reduced of CB efficiency in cMyBP-C$^{-/-}$ (Fig. 1 *C*). Lack of cMyBP-C also induced step-dependent modifications of the CB kinetics. The velocity of CB tilting during the stroke was accelerated by 182% in cMyBP-C$^{-/-}$ compared with cMyBP-C$^{+/+}$ (Fig. 1 *D*, $p < 0.01$) and the duration of the stroke was 62% shorter in cMyBP-C$^{-/-}$ compared with cMyBP-C$^{+/+}$ (2.3 vs. 6.1 ms, respectively, $p < 0.01$). In addition, the overall duration of the CB cycle was 38% shorter in cMyBP-C$^{-/-}$ ($p < 0.01$, Fig. 2 *A*). There was no difference in the maximum rate constant for CB attachment (f_1) between groups (320 ± 60 vs. 276 ± 35 ms^{-1} in cMyBP-C$^{-/-}$ and cMyBP-C$^{+/+}$, respectively). The maximum rate constant for CB detachment (g_2) was 45% lower in cMyBP-C$^{-/-}$ than in cMyBP-C$^{+/+}$ (527 ± 102 vs. 957 ± 131 ms^{-1} respectively, $p < 0.05$). The probability of myosin being weakly bound to actin (P_{A1}) was 60% higher in cMyBP-C$^{-/-}$ than in cMyBP-C$^{+/+}$ (Fig. 2 *B*, $p < 0.001$). However, the probability of a strongly bound, high-force generated state (AM-ADP + Pi state) was reduced by 38% lower in cMyBP-C$^{-/-}$ compared with cMyBP-C$^{+/+}$ (Fig. 2 *C*, $p < 0.001$). In addition, the probability of cycling myosin being in the M-ATP detached state was 134% higher in cMyBP-C$^{-/-}$ than in cMyBP-C$^{+/+}$ hearts (Fig. 2 *D*, $p < 0.001$).

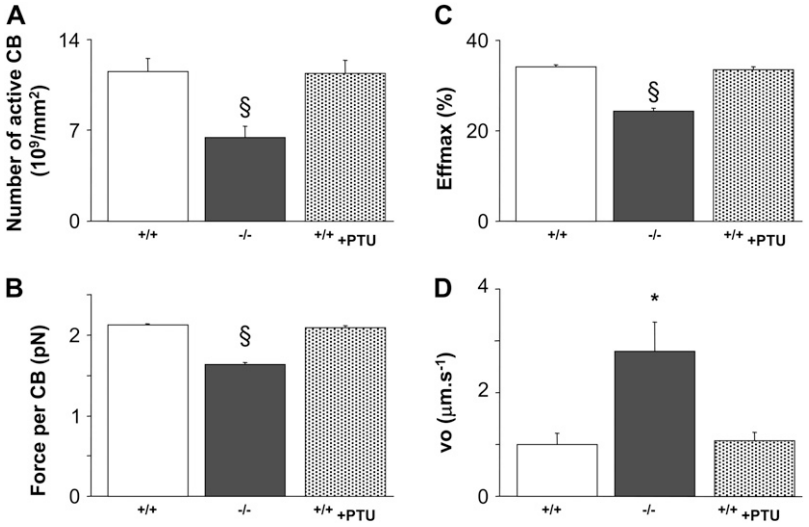

FIGURE 1 Effects of cMyBP-C ablation on CB characteristics. Compared with cMyBP-C$^{+/+}$ ($^{+/+}$), the total number of active CBs (*A*), the unitary force per active CB (*B*), and CB efficiency (Effmax, *C*) were significantly reduced in cMyBP-C$^{-/-}$ ($^{-/-}$). The velocity of the CB during the stroke (v_o, *D*) was higher in cMyBP-C$^{-/-}$. PTU-treated mice ($^{+/+}$+PTU) did not significantly differ from cMyBP-C$^{+/+}$. Values are means ± SE, $N = 8$/group; *$p <$ 0.01; $^{\S}p < 0.001$.

In vitro motility of the myosin CB with actin

cMyBP-C is a known contaminant of purified myosin preparation (32), and significant amount of cMyBP-C was present in the purified myosin solutions as attested by Western-blot analysis (Fig. 3 *A*). Hence, we evaluated the effects of cMyBP-C on actomyosin interactions by analyzing in vitro motility of actin filaments sliding over LV myosin preparation. As compared with cMyBP-C$^{+/+}$, velocity driven by myosin from cMyBP-C$^{-/-}$ was shifted toward lower values, mean velocities being ~18% lower in cMyBP-C$^{-/-}$ than in cMyBP-C$^{+/+}$ (Fig. 4, *A* and *B*, $p < 0.001$). Force produced by myosin was determined by loading actin filaments with α-actinin, an actin-binding protein that acts as an internal load on the force generator (myosin) and impedes the motion of the thin filament (37,38). In both groups, the fraction of mobile filaments linearly decreased by increasing the amount of α-actinin (Fig. 4 *D*). However, the *x* axis intercept of linear regression fits of the data was 60% lower in cMyBP-C$^{-/-}$ than in cMyBP-C$^{+/+}$ (29.1 ± 0.1 vs. 74.4 ± 1.1 μg/ml, respectively, $p < 0.001$), indicating that the lack of cMyBP-C significantly decreased the concentration of α-actinin required to arrest actin filament sliding. This suggests that cMyBP-C improved the force generated per active CB.

Effects of phosphorylation levels of cMyBP-C on the myosin CB

Because phosphorylation/dephosphorylation of cMyBP-C induces rapid and reversible changes in thick filament structure and ordering of myosin heads that possibly modulate the rate of CB cycling (39,40), we next examined the effects of PKA-mediated cMyBP-C phosphorylation on CB mechanics. PKA treatment of cMyBP-C$^{+/+}$ myosin solution induced a 59% increase in cMyBP-C phosphorylation compared with basal values (12.4 ± 1.6 vs. 7.8 ± 1.2 AU, $p <$ 0.001, Fig. 3 *B*). Interestingly, this was associated with a 53%

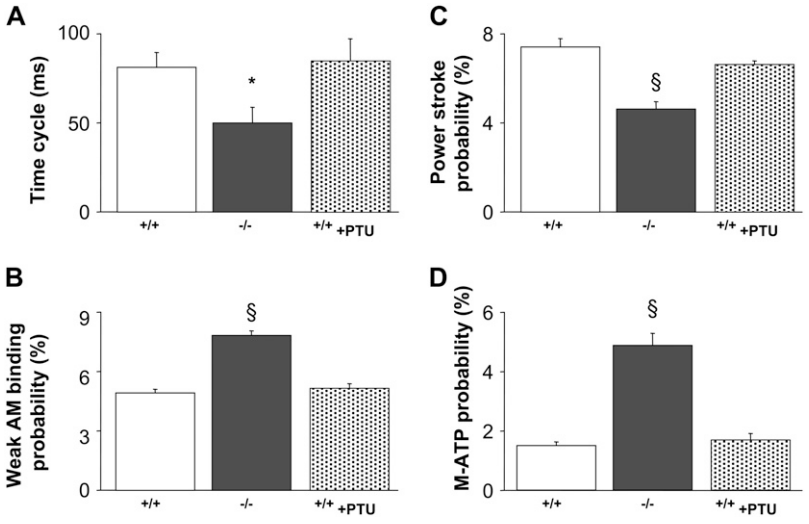

FIGURE 2 Effects of cMyBP-C ablation on kinetics and CB cycle probabilities. Duration of the ATP-ADP-Pi-actomyosin CB cycle (*A*), probability of actomyosin being weakly bound (*B*), strongly bound (*C*) and in the M-ATP detached state (*D*). PTU-treated mice ($^{+/+}$+PTU) did not differ significantly from cMyBP-C$^{+/+}$. Values are means ± SE, $N = 8$/group; *$p < 0.01$, $^{\S}p < 0.001$.

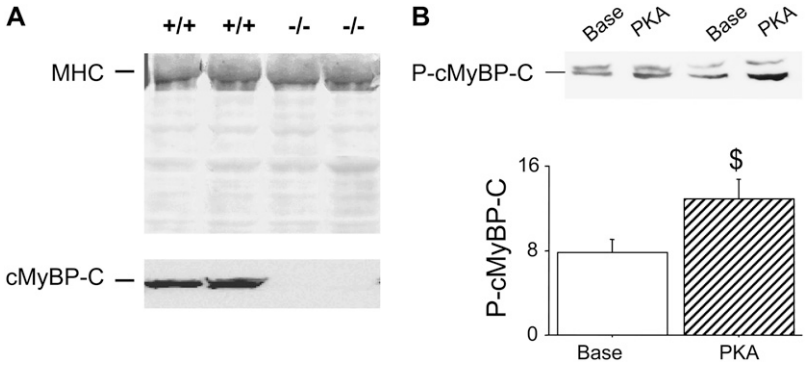

FIGURE 3 Biochemical analyses. (*A*) Typical electrophoresis of myosin solution stained with Coomassie Blue and corresponding immunoblot with the anti-cMyBP-C antibody. cMyBP-C was present in the myosin solution from cMyBP-C$^{+/+}$ ($^{+/+}$) but not in cMyBP-C$^{-/-}$ ($^{-/-}$). (*B*) phosphorylation levels of cMyBP-C before (base) and after PKA treatment (PKA) of cMyBP-C$^{+/+}$ myosin solution. Values are means ± SE, $N = 5$/group; $^{\S}p < 0.001$.

increase in the amount of α-actinin required to arrest thin filament motility (113.6 ± 0.4 vs. 74.4 ± 1.1 μg/ml, respectively, $p < 0.001$; Fig. 4 *D*). Thus, phosphorylation of cMyBP-C induced a significant increase in the force produced by CB, suggesting a specific effect on the power-stroke step. No significant difference in the sliding velocity was observed in PKA-treated myosin (1.98 ± 0.01 μm/s, Fig. 4 *C*) vs. untreated myosin (1.97 ± 0.01 μm/s, Fig. 4 *A*) isolated from cMyBP-C$^{+/+}$.

Potential effects of MHC isoforms on actomyosin interactions

α-MHC represented the major fraction of MHC isoform in cMyBP-C$^{+/+}$ (Fig. 5). cMyBP-C$^{-/-}$ exhibited a +24% increase in the relative expression of β-MHC ($p < 0.001$). There was no significant difference between LV and papillary muscle as regards MHC composition in both groups (data not shown). To determine whether the changes in functional capacities in cMyBP-C$^{-/-}$ were related to a MHC shift, experiments were performed in cMyBP-C$^{+/+}$ mice in which a 25% shift toward β-MHC was induced by a short-term, iodine-deficient, 0.15% 6-*n*-propyl-2-thiouracil (PTU) diet (Fig. 5). Compared with cMyBP-C$^{+/+}$, mechanical and CB properties obtained with papillary muscles did not differ between PTU-treated and untreated cMyBP-C$^{+/+}$ mice (Figs. 1 and 2). Furthermore, no changes in the sliding velocity or in the amount of α-actinin required to arrest thin filament motility were observed between cMyBP-C$^{+/+}$ and PTU-treated mice (data not shown).

DISCUSSION

The sarcomeric cMyBP-C protein is essential for normal cardiac function (7) and its phosphorylation by cAMP-dependent protein kinase (PKA) is an important mechanism that contributes to increased cardiac contractility in response to β-adrenergic stimulation (41–44). Although there is compelling evidence that cMyBP-C influences the activation process of the cardiac sarcomere (12–14,19,45,46), the role

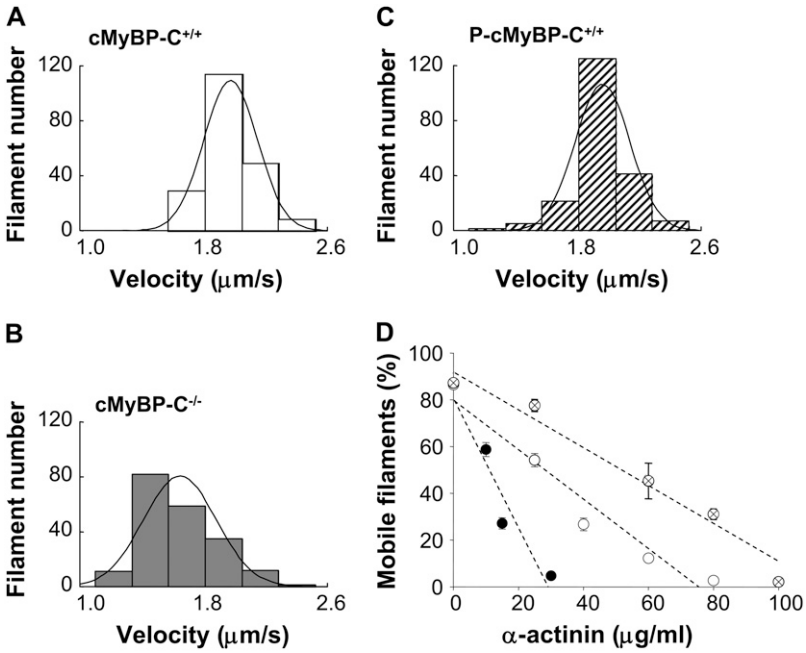

FIGURE 4 Myosin mechanical function. (*A–C*) Distribution of velocities of actin filament sliding over cardiac myosins in cMyBP-C$^{+/+}$ ($^{+/+}$) (*A*), cMyBP-C$^{-/-}$ ($^{-/-}$) (*B*) and after PKA treatment in cMyBP-C$^{+/+}$ (P-cMyBP-C$^{+/+}$) (*C*). Velocities were shifted toward slower values in cMyBP-C$^{-/-}$ compared with cMyBP-C$^{+/+}$ mice. Individual frame-to-frame velocities from tracked filaments are plotted in a frequency histogram; $n = 200$ filaments/group ($N = 6$/group). (*D*) Effects of immobilized α-actinin on fraction of motile actin filaments in cMyBP-C$^{+/+}$ (*open circles*), cMyBP-C$^{-/-}$ (*solid circles*), and after PKA treatment in cMyBP-C$^{+/+}$ (*crossed circles*). The lines are least-squares regression fits: $^{+/+}$: $y = -0.5\,x + 44.6$, $r = 0.73$; $^{-/-}$: $y = -2.8\,x + 80.0$, $r = 0.87$; $^{+/+}$ + PKA: $y = -0.8\,x + 91.7$, $r = 0.93$; and n = at least 100 filaments/α-actinin concentration from three-to-four separate experiments.

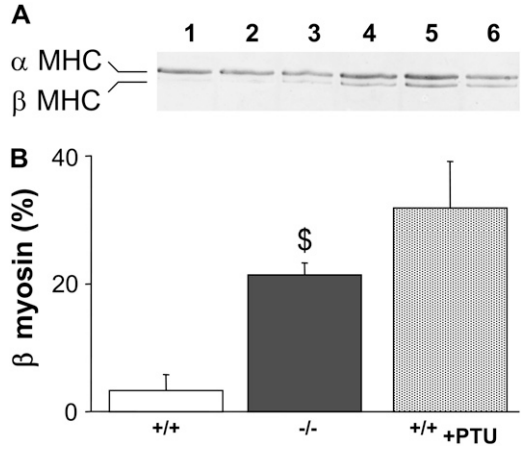

FIGURE 5 Myosin isoform composition. (*A*) Representative electrophoretic separation of LV myosin isoform composition in cMyBP-C$^{+/+}$ (lanes 1–2), cMyBP-C$^{-/-}$ (lanes 3–4), and PTU-treated cMyBP-C$^{+/+}$ mice ($^{+/+}$+PTU) (lanes 5–6). (*B*) Quantitative α- and β-MHC are expressed as means ± SE. N = at least 5/group, $^{\$}p < 0.01$ versus cMyBP-C$^{+/+}$.

of cMyBP-C in contractility and CB cycling remains difficult to discern partly because other myofibrillar proteins, including troponin I, are also targets of PKA-induced phosphorylation. Using a cMyBP-C$^{-/-}$ mouse, we investigated the contribution of cMyBP-C to actin-myosin interactions. The CB model based on A. F. Huxley's original CB model and direct measurements of CB interactions in the in vitro motility assays were analyzed.

In cMyBP-C$^{-/-}$, we found that the probability of myosin being weakly bound to actin was increased, in agreement with earlier predictions that ablation of cMyBP-C increased the likelihood of CB binding (14,19,45). On the basis of a structural model, this has been attributed to the fact that ablation of cMyBP-C reduces the distance between the myosin head and actin binding sites (13), presumably as a result of disrupted binding of cMyBP-C to the S2 domain of myosin (9). Together, these results and data presented herein support the view that the normal role of cMyBP-C is to limit myosin binding to the thin filaments (14,15,47). As a consequence, the increased number of weakly bound CB in cMyBP-C$^{-/-}$ would contribute to the reduced relaxation rate reported both in this study and in previous studies (21,22) given that relaxation rates are limited at least in part by the instantaneous number of bound CBs (22,48). In contrast, during the force generation step, the fraction of CBs in a strongly attached, high force-generated state was severely reduced in cMyBP-C$^{-/-}$ (Figs. 1 and 2). This result is consistent with the reduced CB-dependent stiffness previously reported in myocardium from mice lacking cMyBP-C (49). Given that muscle performance depends on both the number of CBs generating force and the unitary force generated during the power stroke (27), a reduced number of force-generating CBs was a likely explanation for the depressed cardiac performance in cMyBP-C$^{-/-}$ mouse models (20,21). In addition, the increased probability of weakly bound CBs associated with the reduced probability of strongly bound, high-force generated state CB (Fig. 2) indicated that the absence of cMyBP-C impeded the transition from a weak to a strong CB binding to actin. This may explain why that the slow phase of force development, likely representing cooperative CB recruitment, is absent in cMyBP-C$^{-/-}$ myocardium (15). Interestingly, the weak-to-strong binding transition step is associated with conformational changes in myosin CBs (3) that mainly involve swinging of the upper 50 K domain of the myosin head (50,51). As a consequence, the myosin cardiomyopathy loop, containing the first reported FHC missense mutation, comes into contact with the actin surface (50), allowing the actin-myosin CB to stroke. Our data thus raise the possibility that altered CB binding is a common defect that may contribute to the pathophysiology of FHC.

To investigate the force produced during the power-stroke state, we used two independent methods, namely the CB model based on Huxley's equations (24,27) and the in vitro motility assay in the presence of α-actinin, which opposes the motion produced by the swing of the myosin head, thus providing an index of myosin CB force (37,38). The in vitro ability of skeletal heavy meromyosin to support movement of actin filaments has been reported to be modulated by the addition of recombinant N-terminal domains of cMyBP-C, independently of myosin organization into thick filaments (52). Our study extends the prior study by analyzing the effects of native cMyBP-C on cardiac myosin, at baseline, after PKA-induced cMyBP-C phosphorylation and in the presence of α-actinin. Our results indicate that the ability of cardiac myosin to produce force during the power-stroke was markedly reduced in cMyBP-C$^{-/-}$ mice (Figs. 1 *B* and 4 *D*). Therefore, cMyBP-C exerts a controlling influence over CB power-stroke despite the low molar ratio of cMyBP-C to myosin. This was associated with an acceleration of the power-stroke rate, as attested by increased velocity of myosin tilting during the stroke (Fig. 1 *D*). In addition, the total duration of the CB cycle was nearly 40% shorter in cMyBP-C$^{-/-}$ ($p < 0.05$, Fig. 2 *A*), a result in agreement with previous data suggesting that lack of cMyBP-C leads to an accelerated CB cycle (15,17,53). Assuming that one ATP is hydrolyzed per CB cycle (27,50), the normal function of cMyBP-C would be to limit ATP consumption per CB force production cycle. Taken together, these findings strongly suggest that cMyBP-C enhanced the working stroke of myosin and regulated the tuning between the energy release from ATP hydrolysis and the force produced by the tilting of the myosin head during the stroke.

The cMyBP-C phosphorylation level is a potential important regulator of cardiac function. In the absence of cMyBP-C, the ability of the myocardium to respond to β-adrenergic stimulation and the inotropic reserve are significantly diminished (44). Furthermore, a recent study shows that reduced cMyBP-C phosphorylation levels contribute at least in part to the contractile dysfunction of the failing

human heart (36). The precise effects of cMyBP-C phosphorylation levels on contractility and CB cycling have, however, remained difficult to determine because cardiac troponin I and phospholamban are also targets of PKA-induced phosphorylation (9,41). In this study, in vitro assays were performed with unregulated actin filaments, so that the effects of PKA-mediated cMyBP-C phosphorylation could be investigated without the confusing effects on other myofibrillar proteins. We found that the dominant effect of cMyBP-C phosphorylation was to increase the force produced by myosin during the power-stroke (Fig. 4 *D*). Enhanced CB force can be explained by a more favorable position for CB attachment to actin (50,54), which would occur as a consequence of cMyBP-C phosphorylation (9,39). Thus, although both ablation of cMyBP-C and its phosphorylation critically regulate the distance between the myosin heads and the actin binding sites, only phosphorylation of cMyBP-C would improve the orientation of the myosin head in relation to actin. Taken as a whole, our data provide new insights into the molecular mechanism by which PKA-mediated phosphorylation of cMyBP-C controls myocardium-enhanced cardiac function in response to β-adrenergic stimulation.

Furthermore, we found that both unloaded muscle shortening and myosin sliding velocities were reduced in cMyBP-C$^{-/-}$. These changes could not be attributed to the moderate increased in the slow, β-myosin isoform composition, given that PTU-induced similar shift in the myosin isoform pattern did not modify these parameters (Fig. 5). Alternatively, ablation of cMyBP-C may conceivably reduce sliding velocity due to a slower transition rate from the weakly to the strongly attached actomyosin state (55,56).

Mechanical parameters were obtained from LV papillary muscles. This raises questions as to whether some of the observed data reflected the more general ventricular muscle. However, no significant difference between papillary muscle and whole LV was observed in regard to MHC composition. Moreover, results obtained from in motility assays, i.e., at constant number of myosin molecules per surface area, clearly support papillary muscle experiments. Therefore, impaired CB properties could not be attributed to potential heterogeneity in the distribution of myosin isoforms or in cardiac fibrosis.

Mouse models in which cMyBP-C has been knocked out by homologous recombination, leading to deletion of the entire coding sequence (16) or the transcription initiation site (21), provide powerful tools to enable us to better understand the role of cMyBP-C in myocardial contraction. However, consistent with the absence of cMyBP-C, physiological studies demonstrated contractile deficits and hypertrophy of the hearts in the mutant mice (16,20,21,53,57). Therefore, it is possible that some of the observed data in our cMyBP-C-null mouse model are related to hypertrophic remodeling rather than to cMyBP-C ablation. In addition, because cMyBP-C is expressed at gestation day 8 in mice (58), cardiac remodeling may begin at an early stage in mammalian cardiac development. However, the phenotype of the present homozygous mice is identical to what was observed in a similar deficient cMyBP-C mouse model (16) and in homozygous cMyBP-Ct/t (59). Moreover, cMyBP-C-null mice are well-established, widely-used models to analyze the structural and functional consequences of cMyBP-C ablation (15,16,18,20,21,53,57). It is notable that our study was performed with native cMyBP-C. Therefore, interactions of N-terminal domain of the cMyBP-C with either or both actin and myosin could potentially influence discrete steps in the CB cycle. Further studies are needed to precise the molecular mechanisms by which the different regions of cMyBP-C affects CB interactions.

In conclusion, we find that cMyBP-C slows the overall CB cycle duration, confirming early studies (15,17,20,57). Our data provide new insights into the specific steps at which cMyBP-C regulates actin-myosin cycle and how potential modifications of the myosin CB cycle contribute to the cardiac dysfunction. Importantly, we find that cMyBP-C prevents inefficient weakly bound CBs, enhances transition from weakly bound to strongly bound CBs and increases force produced during the power stroke. Moreover, CB force production can be majored by PKA-based phosphorylation of cMyBP-C. Thus, cMyBP-C is likely to play a significant role in regulating the fine molecular tuning of the myosin CB.

This study was supported in part by grants from the Association Française Contre les Myopathies, from the Institut National de la Santé et de la Recherche Médicale (No. PNRMC-A04048DS), and by the sixth Framework Program of the European Union (No. Marie Curie EXT-014051).

REFERENCES

1. Lecarpentier, Y., F. X. Blanc, J. Quillard, J. L. Hebert, X. Krokidis, and C. Coirault. 2005. Statistical mechanics of myosin molecular motors in skeletal muscles. *J. Theor. Biol.* 235:381–392.
2. Lymn, R. W., and E. W. Taylor. 1971. Mechanism of adenosine triphosphate hydrolysis by actomyosin. *Biochemistry.* 10:4617–4624.
3. Geeves, M. A., and P. B. Conibear. 1995. The role of three-state docking of myosin S1 with actin in force generation. *Biophys. J.* 68: 194S–199S.
4. Spudich, J. A. 2001. The myosin swinging cross-bridge model. *Nature Rev. Mol. Cell Biol.* 2:387–392.
5. Gordon, A. M., E. Homsher, and M. Regnier. 2000. Regulation of contraction in striated muscle. *Physiol. Rev.* 80:853–924.
6. Tardiff, J. C. 2005. Sarcomeric proteins and familial hypertrophic cardiomyopathy: linking mutations in structural proteins to complex cardiovascular phenotypes. *Heart Fail. Rev.* 10:237–248.
7. Flashman, E., C. Redwood, J. Moolman-Smook, and H. Watkins. 2004. Cardiac myosin binding protein C: its role in physiology and disease. *Circ. Res.* 94:1279–1289.
8. Gruen, M., and M. Gautel. 1999. Mutations in β-myosin S2 that cause familial hypertrophic cardiomyopathy (FHC) abolish the interaction with the regulatory domain of myosin-binding protein-C. *J. Mol. Biol.* 286:933–949.
9. Gautel, M., O. Zuffardi, A. Freiburg, and S. Labeit. 1995. Phosphorylation switches specific for the cardiac isoform of myosin binding protein-C: a modulator of cardiac contraction? *EMBO J.* 14:1952–1960.

10. Freiburg, A., and M. Gautel. 1996. A molecular map of the interactions between titin and myosin-binding protein C. Implications for sarcomeric assembly in familial hypertrophic cardiomyopathy. *Eur. J. Biochem. FEBS*. 235:317–323.

11. Kulikovskaya, I., G. McClellan, J. Flavigny, L. Carrier, and S. Winegrad. 2003. Effect of MyBP-C binding to actin on contractility in heart muscle. *J. Gen. Physiol.* 122:761–774.

12. Moss, R. L. 1986. Effects on shortening velocity of rabbit skeletal muscle due to variations in the level of thin-filament activation. *J. Physiol.* 377:487–505.

13. Hofmann, P. A., H. C. Hartzell, and R. L. Moss. 1991. Alterations in Ca^{2+} sensitive tension due to partial extraction of C-protein from rat skinned cardiac myocytes and rabbit skeletal muscle fibers. *J. Gen. Physiol.* 97:1141–1163.

14. Herron, T. J., E. Rostkova, G. Kunst, R. Chaturvedi, M. Gautel, and J. C. Kentish. 2006. Activation of myocardial contraction by the N-terminal domains of myosin binding protein-C. *Circ. Res.* 98:1290–1298.

15. Stelzer, J. E., J. R. Patel, and R. L. Moss. 2006. Protein kinase A-mediated acceleration of the stretch activation response in murine skinned myocardium is eliminated by ablation of cMyBP-C. *Circ. Res.* 99:884–890.

16. Harris, S. P., C. R. Bartley, T. A. Hacker, K. S. McDonald, P. S. Douglas, M. L. Greaser, P. A. Powers, and R. L. Moss. 2002. Hypertrophic cardiomyopathy in cardiac myosin binding protein-C knockout mice. *Circ. Res.* 90:594–601.

17. Korte, F. S., K. S. McDonald, S. P. Harris, and R. L. Moss. 2003. Loaded shortening, power output, and rate of force redevelopment are increased with knockout of cardiac myosin binding protein-C. *Circ. Res.* 93:752–758.

18. Cazorla, O., S. Szilagyi, N. Vignier, G. Salazar, E. Kramer, G. Vassort, L. Carrier, and A. Lacampagne. 2006. Length and protein kinase A modulations of myocytes in cardiac myosin binding protein C-deficient mice. *Cardiovasc. Res.* 69:370–380.

19. Stelzer, J. E., S. B. Dunning, and R. L. Moss. 2006. Ablation of cardiac myosin-binding protein-C accelerates stretch activation in murine skinned myocardium. *Circ. Res.* 98:1212–1218.

20. Harris, S. P., E. Rostkova, M. Gautel, and R. L. Moss. 2004. Binding of myosin binding protein-C to myosin subfragment S2 affects contractility independent of a tether mechanism. *Circ. Res.* 95:930–936.

21. Carrier, L., R. Knoll, N. Vignier, D. I. Keller, P. Bausero, B. Prudhon, R. Isnard, M. L. Ambroisine, M. Fiszman, J. Ross, Jr., K. Schwartz, and K. R. Chien. 2004. Asymmetric septal hypertrophy in heterozygous cMyBP-C null mice. *Cardiovasc. Res.* 63:293–304.

22. Pohlmann, L., I. Kroger, N. Vignier, S. Schlossarek, E. Kramer, C. Coirault, K. R. Sultan, A. El-Armouche, S. Winegrad, T. Eschenhagen, and L. Carrier. 2007. Cardiac myosin-binding protein C is required for complete relaxation in intact myocytes. *Circ. Res.* 101:928–938.

23. Guellich, A., T. Damy, Y. Lecarpentier, M. Conti, V. Claes, J. L. Samuel, J. Quillard, J. L. Hebert, T. Pineau, and C. Coirault. 2007. Role of oxidative stress in cardiac dysfunction of PPAR$\alpha^{-/-}$ mice. *Am. J. Physiol.* 293:H93–H102.

24. Lecarpentier, Y., D. Chemla, F. X. Blanc, J. C. Pourny, T. Joseph, B. Riou, and C. Coirault. 1998. Mechanics, energetics, and crossbridge kinetics of rabbit diaphragm during congestive heart failure. *FASEB J.* 12:981–989.

25. Li, L., J. Desantiago, G. Chu, E. G. Kranias, and D. M. Bers. 2000. Phosphorylation of phospholamban and troponin I in β-adrenergic-induced acceleration of cardiac relaxation. *Am. J. Physiol.* 278:H769–H779.

26. Woledge, R. C., N. A. Curtin, and E. Homsher. 1985. Energetic aspects of muscle contraction. *Monogr. Physiol. Soc.* 41:1–357.

27. Huxley, A. F. 1957. Muscle structure and theories of contraction. *Prog. Biophys. Biophys. Chem.* 7:255–318.

28. Eisenberg, E., T. L. Hill, and Y. Chen. 1980. Crossbridge model of muscle contraction. Quantitative analysis. *Biophys. J.* 29:195–227.

29. Coirault, C., F. Lambert, T. Joseph, F. X. Blanc, D. Chemla, and Y. Lecarpentier. 1997. Developmental changes in crossbridge properties and myosin isoforms in hamster diaphragm. *Am. J. Respir. Crit. Care Med.* 156:959–967.

30. Molloy, J. E., J. E. Burns, J. Kendrick-Jones, R. T. Tregear, and D. C. White. 1995. Movement and force produced by a single myosin head. *Nature*. 378:209–212.

31. Keller, D. I., C. Coirault, T. Rau, T. Cheav, M. Weyand, K. Amann, Y. Lecarpentier, P. Richard, T. Eschenhagen, and L. Carrier. 2004. Human homozygous R403W mutant cardiac myosin presents disproportionate enhancement of mechanical and enzymatic properties. *J. Mol. Cell. Cardiol.* 36:355–362.

32. Starr, R., and G. Offer. 1971. Polypeptide chains of intermediate molecular weight in myosin preparations. *FEBS Lett.* 15:40–44.

33. Pardee, J. D., and J. A. Spudich. 1982. Purification of muscle actin. *Methods Enzymol.* 85:164–181.

34. Agbulut, O., A. Huet, N. Niederlander, M. Puceat, P. Menasche, and C. Coirault. 2007. Green fluorescent protein impairs actin-myosin interactions by binding to the actin-binding site of myosin. *J. Biol. Chem.* 282:10465–10471.

35. Sellers, J. R., G. Cuda, F. Wang, and E. Homsher. 1993. Myosin-specific adaptations of the motility assay. *Methods Cell Biol.* 39:23–49.

36. El-Armouche, A., L. Pohlmann, S. Schlossarek, J. Starbatty, Y. H. Yeh, S. Nattel, D. Dobrev, T. Eschenhagen, and L. Carrier. 2007. Decreased phosphorylation levels of cardiac myosin-binding protein-C in human and experimental heart failure. *J. Mol. Cell. Cardiol.* 43: 223–229.

37. VanBuren, P., S. L. Alix, J. A. Gorga, K. J. Begin, M. M. LeWinter, and N. R. Alpert. 2002. Cardiac troponin T isoforms demonstrate similar effects on mechanical performance in a regulated contractile system. *Am. J. Physiol.* 282:H1665–H1671.

38. Foster, D. B., T. Noguchi, P. VanBuren, A. M. Murphy, and J. E. Van Eyk. 2003. C-terminal truncation of cardiac troponin I causes divergent effects on ATPase and force: implications for the pathophysiology of myocardial stunning. *Circ. Res.* 93:917–924.

39. Weisberg, A., and S. Winegrad. 1996. Alteration of myosin cross-bridges by phosphorylation of myosin-binding protein C in cardiac muscle. *Proc. Natl. Acad. Sci. USA*. 93:8999–9003.

40. Sadayappan, S., J. Gulick, H. Osinska, L. A. Martin, H. S. Hahn, G. W. Dorn 2nd, R. Klevitsky, C. E. Seidman, J. G. Seidman, and J. Robbins. 2005. Cardiac myosin-binding protein-C phosphorylation and cardiac function. *Circ. Res.* 97:1156–1163.

41. Garvey, J. L., E. G. Kranias, and R. J. Solaro. 1988. Phosphorylation of C-protein, troponin I and phospholamban in isolated rabbit hearts. *Biochem. J.* 249:709–714.

42. Schlender, K. K., and L. J. Bean. 1991. Phosphorylation of chicken cardiac C-protein by calcium/calmodulin-dependent protein kinase II. *J. Biol. Chem.* 266:2811–2817.

43. Hartzell, H. C., and D. B. Glass. 1984. Phosphorylation of purified cardiac muscle C-protein by purified cAMP-dependent and endogenous Ca^{2+}-calmodulin-dependent protein kinases. *J. Biol. Chem.* 259:15587–15596.

44. Brickson, S., D. P. Fitzsimons, L. Pereira, T. Hacker, H. Valdivia, and R. L. Moss. 2007. In vivo left ventricular functional capacity is compromised in cMyBP-C null mice. *Am. J. Physiol.* 292:H1747–H1754.

45. Moss, R. L. 1992. Ca^{2+} regulation of mechanical properties of striated muscle. Mechanistic studies using extraction and replacement of regulatory proteins. *Circ. Res.* 70:865–884.

46. de Tombe, P. P. 2006. Myosin binding protein C in the heart. *Circ. Res.* 98:1234–1236.

47. Sadayappan, S., H. Osinska, R. Klevitsky, J. N. Lorenz, M. Sargent, J. D. Molkentin, C. E. Seidman, J. G. Seidman, and J. Robbins. 2006. Cardiac myosin binding protein C phosphorylation is cardioprotective. *Proc. Natl. Acad. Sci. USA*. 103:16918–16923.

48. Brutsaert, D. L., and S. U. Sys. 1989. Relaxation and diastole of the heart. *Physiol. Rev.* 69:1228–1315.

49. Palmer, B. M., B. K. McConnell, G. H. Li, C. E. Seidman, J. G. Seidman, T. C. Irving, N. R. Alpert, and D. W. Maughan. 2004. Reduced crossbridge dependent stiffness of skinned myocardium from mice lacking cardiac myosin binding protein-C. *Mol. Cell. Biochem.* 263:73–80.

50. Holmes, K. C., and R. R. Schroder. 2003. Switch 1 opens on strong binding to actin. Molecular and cellular aspects of muscle contraction. *Adv. Exp. Med. Biol.* 538:159–166.

51. Rayment, I., H. M. Holden, M. Whittaker, C. B. Yohn, M. Lorenz, K. C. Holmes, and R. A. Milligan. 1993. Structure of the actin-myosin complex and its implications for muscle contraction. *Science.* 261:58–65.

52. Razumova, M. V., J. F. Shaffer, A. Y. Tu, G. V. Flint, M. Regnier, and S. P. Harris. 2006. Effects of the N-terminal domains of myosin binding protein-C in an in vitro motility assay: evidence for long-lived crossbridges. *J. Biol. Chem.* 281:35846–35854.

53. Palmer, B. M., D. Georgakopoulos, P. M. Janssen, Y. Wang, N. R. Alpert, D. F. Belardi, S. P. Harris, R. L. Moss, P. G. Burgon, C. E. Seidman, J. G. Seidman, D. W. Maughan, and D. A. Kass. 2004. Role of cardiac myosin binding protein C in sustaining left ventricular systolic stiffening. *Circ. Res.* 94:1249–1255.

54. Molloy, J. E., J. E. Burns, J. C. Sparrow, R. T. Tregear, J. Kendrick-Jones, and D. C. White. 1995. Single-molecule mechanics of heavy meromyosin and S1 interacting with rabbit or *Drosophila* actins using optical tweezers. *Biophys. J.* 68:298S–305S.

55. Stehle, R., and B. Brenner. 2000. Crossbridge attachment during high-speed active shortening of skinned fibers of the rabbit psoas muscle: implications for crossbridge action during maximum velocity of filament sliding. *Biophys. J.* 78:1458–1473.

56. Cuda, G., E. Pate, R. Cooke, and J. R. Sellers. 1997. In vitro actin filament sliding velocities produced by mixtures of different types of myosin. *Biophys. J.* 72:1767–1779.

57. Stelzer, J. E., D. P. Fitzsimons, and R. L. Moss. 2006. Ablation of myosin-binding protein-C accelerates force development in mouse myocardium. *Biophys. J.* 90:4119–4127.

58. Fougerousse F., A. L. Delezoide, M. Y. Fiszman, K. Schwartz, J. S. Bechmann, and L. Carrier. 1998. Cardiac myosin binding protein C gene is specifically expressed in heart during murine and human development. *Circ. Res.* 82:130–133.

59. McConnell, B. K., K. A. Jones, D. Fatkin, L. H. Arroyo, R. T. Lee, O. Aristizabal, D. H. Turnbull, D. Georgakopoulos, D. Kass, M. Bond, H. Niimura, F. J. Schoen, D. Conner, D. A. Fischman, C. E. Seidman, and J. G. Seidman. 1999. Dilated cardiomyopathy in homozygous myosin-binding protein-C mutant mice. *J. Clin. Invest.* 104:1235–1244.